

Hybrid Monte Carlo-Molecular Dynamics Framework for Silica Polymerization: Bridging Short-Timescale Reactions with Long-Range Structural Ordering

Haoran Liu¹ and Xinyi Chen²

¹Yunnan Minzu University, Department of Chemical Engineering, 134 Yiwen Road, Chenggong District, Kunming, Yunnan, China

²Jiangxi University of Science and Technology, Department of Chemical Engineering, 86 Hongqi Avenue, Ganzhou, Jiangxi, China

Abstract

Silica polymerization remains a critical process in materials science, yet its multiscale nature challenges conventional modeling approaches. This work presents a hybrid computational framework combining kinetic Monte Carlo (kMC) and reactive molecular dynamics (MD) to simulate silica network formation under aqueous conditions. The kMC module governs stochastic reaction kinetics, including hydrolysis ($\text{Si-O-Si} + \text{H}_2\text{O} \rightleftharpoons 2\text{Si-OH}$) and condensation ($\text{Si-OH} + \text{HO-Si} \rightarrow \text{Si-O-Si} + \text{H}_2\text{O}$), with rates modulated by local proton activity (a_{H^+}). The MD component employs the ReaxFF force field to resolve atomic-scale structural relaxation and stress accumulation (σ_{ij}) in SiO_4 tetrahedra. A bidirectional coupling protocol synchronizes kMC and MD domains via a weighted Hamiltonian $H = \lambda H_{\text{kMC}} + (1 - \lambda)H_{\text{MD}}$, where λ adaptively scales with the system's tetrahedrality parameter ($\langle Q^4 \rangle$). The framework introduces a time-decomposition algorithm to handle disparate timescales, with kMC advancing reaction steps ($\Delta t_{\text{kMC}} \sim 10^{-6}$ s) and MD resolving picosecond-scale vibrations ($\Delta t_{\text{MD}} = 0.5$ fs). Validation against silica solubility curves ($\log[\text{SiO}_2]_{\text{sat}} = -0.38 \cdot \text{pH} + 3.2$) and small-angle neutron scattering (SANS) data reveals consistent oligomer size distributions (radius of gyration $R_g = 1.2\lambda 2.8$ nm). However, discrepancies emerge in gelation times (t_g), with simulations overestimating experiments by 18–22% at $\text{pH} > 5$, suggesting incomplete treatment of hydrogen-bonding networks. The model identifies metastable Q^3 -rich clusters as kinetic traps, delaying percolation thresholds. This work highlights the necessity of explicit solvent modeling and strain-dependent rate corrections in multiscale silica polymerization frameworks.

POLAR PUBLICATIONS © This document is licensed under the Creative Commons Attribution 4.0 International License (CC BY 4.0). Under the terms of this license, you are free to share, copy, distribute, and transmit the work in any medium or format, and to adapt, remix, transform, and build upon the work for any purpose, even commercially, provided that appropriate credit is given to the original author(s), a link to the license is provided, and any changes made are indicated. To view a copy of this license, visit <http://creativecommons.org/licenses/by/4.0/>.

1. Introduction

Silicate networks form through a hierarchy of processes that span a vast range of time and length scales. Proton transfer events occur at femtosecond scales, molecular rearrangements are observed on the order of picoseconds, and oligomer aggregation can extend into the millisecond regime. This complex multiscale behavior poses significant challenges for traditional computational models. Classical theories such as Smoluchowski aggregation or density functional theory (DFT)-based reaction pathways have provided valuable insights into individual aspects of network formation, yet they fail to bridge the gap between these disparate scales effectively. In particular, while reactive molecular dynamics (MD) simulations employing force fields such as ReaxFF have the capacity to capture bond-breaking and bond-forming events with atomic resolution, they are inherently limited by the short timescales accessible in simulations. Rare events, such as the slow polymerization reactions that occur over time scales on the order of 10^3 seconds, remain out of reach for conventional MD simulations due to prohibitive computational costs [1], [2].

A major challenge in modeling silicate network formation is the necessity of accurately capturing both short-range covalent interactions and long-range network organization. Bond formation in silicate systems involves concerted mechanisms that include hydrolysis, condensation, and complexation with various counterions. The energetics and kinetics of these elementary steps are significantly influenced by solvation effects, pH variations, and the presence of external templates or additives that can modulate reaction pathways. Traditional DFT ap-

proaches provide atomistic insights into reaction barriers and intermediate species; however, their applicability is confined to relatively small system sizes and short time windows. On the other hand, classical force fields can describe large-scale structural evolution but lack the ability to explicitly model reactive events without the incorporation of empirical reaction coordinates. These limitations necessitate the development of hybrid computational strategies that integrate quantum mechanical calculations with coarse-grained or mesoscopic models to extend temporal and spatial resolutions.

Recent advances in machine learning (ML)-augmented force fields have shown promise in addressing the limitations of conventional computational techniques. By training neural network potentials on high-fidelity quantum chemical datasets, researchers have developed reactive potentials that retain the accuracy of DFT calculations while achieving computational efficiencies comparable to classical MD simulations. Such ML-based methods have demonstrated significant improvements in predicting the formation of silicate oligomers and their subsequent polymerization dynamics. Furthermore, enhanced sampling techniques such as metadynamics, accelerated MD, and replica exchange methods have been employed to access rare-event kinetics in silicate network evolution. These approaches enable the exploration of reaction pathways that are otherwise inaccessible due to energy barriers and long relaxation times [3].

One of the primary factors governing silicate polymerization is the distribution of oligomeric species within solution, which is dictated by both thermodynamic stability and kinetic accessibility. Experimental studies employing nuclear magnetic res-

Silicate Oligomer	Structure Type	Formation Energy (kJ/mol)	Dominant Regime	pH
Monomer (SiO_4^{4-})	Tetrahedral	0 (reference)	Alkaline	
Dimer ($\text{Si}_2\text{O}_7^{6-}$)	Corner-sharing tetrahedra	-45.2	Alkaline	
Cyclic Trimer ($\text{Si}_3\text{O}_9^{6-}$)	Three-membered ring	-72.5	Neutral to alkaline	
Linear Trimer ($\text{Si}_3\text{O}_{10}^{8-}$)	Linear chain	-68.3	Alkaline	
Cyclic Tetramer ($\text{Si}_4\text{O}_{12}^{8-}$)	Four-membered ring	-98.7	Neutral	
3D Oligomers	Polyhedral clusters	Variable	Near-neutral to acidic	

Table 1. Comparison of silicate oligomer structures, their relative formation energies, and the dominant pH regime in which they are observed.

onance (NMR) spectroscopy and small-angle X-ray scattering (SAXS) have revealed that the formation of silicate oligomers proceeds through a complex interplay between monomer addition and cluster rearrangement. In highly alkaline conditions, soluble silicate species predominantly exist as small, negatively charged oligomers, while under near-neutral conditions, the system undergoes a gradual transition toward three-dimensional network formation. These experimental insights provide critical benchmarks for validating computational models and refining force field parameterizations [4].

To illustrate the diversity of silicate oligomer structures, we present a summary of the most commonly observed species along with their associated formation energies as computed from DFT-based calculations. The table below provides a comparative analysis of different silicate clusters, highlighting the relative stability of various configurations [5], [6].

Beyond the oligomeric stage, the self-assembly of extended silicate networks follows a nucleation-and-growth mechanism that is highly dependent on supersaturation conditions, ionic strength, and the presence of structure-directing agents. The competition between kinetic trapping and thermodynamic stability leads to the formation of metastable intermediates that subsequently undergo reorganization into more stable configurations. Molecular simulations have indicated that the free energy landscape of silicate polymerization is punctuated by multiple intermediate states corresponding to partially condensed species. The presence of water plays a crucial role in mediating these transitions, as hydrolysis and condensation reactions are both influenced by local hydration shell dynamics.

Another critical aspect of silicate network formation is the role of counterions in modulating polymerization pathways. Cations such as sodium, potassium, and calcium interact with negatively charged silicate species, thereby stabilizing certain configurations and altering reaction kinetics. Spectroscopic studies have demonstrated that alkali metal cations preferentially coordinate with terminal oxygen atoms in silicate oligomers, leading to variations in bond angles and network connectivity. Computationally, these effects have been captured through explicit solvation models that incorporate ion-silicate interactions in a self-consistent manner.

To provide a quantitative understanding of cation effects, we present a computational study comparing the binding energies of various cations with silicate oligomers. The data in Table 2 illustrate the significant influence of counterion identity on silicate stabilization.

Kinetic Monte Carlo (kMC) methods, when parameterized using bulk activation energies (E_a), offer an alternative means to simulate long-time behavior. However, these methods often neglect local strain effects and subtle variations in the reaction environment, which can lead to inaccurate predictions of cluster morphology and network evolution. Recent attempts to couple kMC and MD simulations have shown promise in combining the strengths of both approaches, yet these efforts frequently encounter synchronization challenges, particularly in preserving detailed balance during the exchange of configurations between the two solvers. Such issues can compromise the accuracy and reliability of the simulation outcomes.

This work addresses these challenges by introducing a novel hybrid kMC-MD framework that couples stochastic reaction kinetics with atomistic detail. Our approach incorporates three key innovations. First, we implement a reaction-diffusion kernel for the kMC component that dynamically updates rate constants based on MD-derived strain tensors (ϵ_{ij}). This coupling allows local mechanical effects, which are often overlooked in conventional kMC models, to be directly integrated into the reaction kinetics. Second, a solvent-mediated proton transport model is incorporated, capturing the intricacies of the Grotthuss mechanism. This feature is essential for accurately simulating the early-stage proton transfer kinetics that dominate silicate polymerization. Third, a graph-theoretic analysis of the evolving silica network is employed to quantify cyclic defect densities (n_{ring}) and to characterize the connectivity of the system.

Benchmarking our model against experimental ^{29}Si nuclear magnetic resonance (NMR) spectra reveals that the predicted Q^4/Q^3 ratio is improved significantly, with errors reduced to less than 9% compared to over 27% in models relying solely on kMC. Furthermore, the framework demonstrates robust utility in modeling nanoporous silica formation, with simulated pore size distributions ($d_p = 2\text{--}5$ nm) aligning with nitrogen adsorption experiments within an error margin of 15%.

The remainder of this paper is organized as follows. In Section 2, we describe the computational methodology, detailing the partitioning of the simulation domain into subdomains assigned to either kMC or MD, the use of a face-centered cubic (FCC) lattice for the kMC model, and the specifics of the MD simulations including the ReaxFF-SiO₂ parameterization and long-range Coulomb interaction treatments. Section 3 focuses on the reaction network and the role of solvent effects, discussing the pH-dependent proton transfer kinetics, the incor-

Cation	Preferred Binding Site	Binding Energy (kJ/mol)	Effect on Polymerization
Na ⁺	Terminal oxygen	-65.3	Moderate stabilization
K ⁺	Bridging oxygen	-58.7	Weak stabilization
Ca ²⁺	Multiple coordination sites	-120.5	Strong stabilization
Mg ²⁺	Inner coordination shell	-135.2	Very strong stabilization
Al ³⁺	Framework incorporation	-210.4	Structural reinforcement

Table 2. Binding energies of various cations to silicate oligomers, illustrating their effects on polymerization stability.

poration of coarse-grained water dynamics, and the modeling of hydronium ion transport via the Grotthuss mechanism. Section 4 elaborates on the structural evolution of the system and the gelation dynamics that govern network formation, including detailed analyses of cluster aggregation, fractal dimension evolution, and the impact of cyclic silicate motifs on network stiffness. Finally, Section 5 presents our conclusions, summarizes the key findings, discusses limitations, and outlines avenues for future research. This comprehensive treatment of silica polymerization, achieved by integrating both microscopic and mesoscopic phenomena, represents a significant step toward the predictive modeling of complex silicate-based materials.

2. Computational Methodology

The hybrid simulation framework developed in this work is designed to seamlessly integrate kinetic Monte Carlo (kMC) methods with molecular dynamics (MD) simulations, thereby capturing the essential physics of silicate polymerization across a broad range of time scales. The computational domain is partitioned into N subdomains, with each subdomain dynamically assigned to either the kMC or MD solver based on a local reaction density threshold, ρ_c . Specifically, when the local density of reactive species exceeds $\rho_c = 0.15 \text{ nm}^{-3}$, the corresponding subdomain is advanced using MD; otherwise, the kMC method is employed. This partitioning strategy ensures that computational resources are allocated efficiently, with MD capturing fast, atomistically detailed processes and kMC handling slower, statistically driven events [7].

The MD component of the hybrid simulation employs a reactive force field (ReaxFF) to model bond formation and breakage with high fidelity. ReaxFF has been extensively parameterized for silicate systems and is capable of capturing key reaction mechanisms, including hydrolysis, condensation, and the stabilization of intermediate oligomers. The time step for MD simulations is set to 0.25 fs to ensure accurate integration of atomic forces, while periodic boundary conditions are applied to maintain consistency across subdomains. The kMC component, on the other hand, employs a graph-based representation of silicate species, where reaction probabilities are computed based on pre-tabulated activation barriers obtained from density functional theory (DFT) calculations. By leveraging this hierarchical approach, the simulation framework is able to bridge the time-scale gap inherent in silicate network evolution.

One of the key advantages of this hybrid methodology is its ability to adaptively resolve reaction kinetics without incurring prohibitive computational costs. In regions where reactive events are frequent, the system transitions to MD to accurately capture short-range atomic interactions. Conversely, in sparsely reactive regions, kMC efficiently propagates the system forward without requiring explicit atomic trajectories. This adaptive approach is particularly useful in studying the competition between oligomerization and gelation, where localized fluctuations in reaction rates can give rise to heterogeneous network structures [8].

To evaluate the efficiency of this hybrid approach, we performed benchmark simulations on a model silicate solution containing a controlled distribution of monomers and oligomers. The performance metrics, including computational speedup and accuracy relative to full MD simulations, are summarized in Table 3. The results demonstrate that the hybrid framework achieves a substantial reduction in computational cost while maintaining high fidelity in the predicted oligomer size distribution.

The results indicate that the hybrid framework achieves a nearly sevenfold acceleration in simulation time compared to full MD, with only a minor deviation in predicted oligomer distributions. This improvement is particularly valuable for studying long-time-scale phenomena, such as gelation and network percolation, which are otherwise intractable with traditional MD approaches alone.

Beyond efficiency, another critical feature of the hybrid framework is its ability to capture the emergence of mesoscale structural motifs in silicate networks. As polymerization proceeds, the system transitions from a regime dominated by isolated oligomers to an interconnected gel-like network. This process is governed by a balance between reaction kinetics and diffusion-limited aggregation, both of which are naturally accommodated within the hybrid scheme. The competition between these mechanisms leads to a broad distribution of network topologies, ranging from loosely branched structures to densely cross-linked frameworks.

To quantify the degree of network connectivity, we introduce a graph-based order parameter, ξ , which measures the fraction of fully coordinated silicate species within the system. Specifically, ξ is defined as:

$$\xi = \frac{N_{\text{coordinated}}}{N_{\text{total}}}$$

where $N_{\text{coordinated}}$ represents the number of silicate species

Simulation Method	Average Computational Time (per ns)	Accuracy (% deviation from full MD)	Speedup Factor
Full MD (ReaxFF)	120 hrs	Reference (0%)	1.0
kMC-only	5 hrs	15.7%	24.0
Hybrid (MD + kMC)	18 hrs	3.2%	6.7

Table 3. Comparison of computational efficiency and accuracy for different simulation methods applied to silicate polymerization.

Simulation Method	ξ at 1 ns	ξ at 10 ns	ξ at 50 ns	ξ at 100 ns
Full MD (ReaxFF)	0.12	0.45	0.78	0.92
kMC-only	0.10	0.38	0.65	0.81
Hybrid (MD + kMC)	0.11	0.42	0.74	0.89

Table 4. Evolution of network connectivity parameter ξ over time for different simulation methods.

with four or more bridging oxygen bonds, and N_{total} is the total number of silicate units. The evolution of ξ over time for different simulation methods is presented in Table 4.

These results confirm that the hybrid framework closely reproduces the network evolution predicted by full MD, with minor discrepancies at intermediate time scales. Importantly, the hybrid approach significantly outperforms kMC-only simulations in capturing early-stage oligomerization dynamics, highlighting the necessity of retaining atomistic resolution in regions of high reaction density.

The kMC component utilizes a face-centered cubic (FCC) grid with a lattice spacing of $a = 0.76$ nm. Each lattice site is capable of hosting $\text{Si}(\text{OH})_m$ species, where m can assume values of 3 or 4, corresponding to different coordination environments [9]. Transition rates between sites, denoted $k_{i \rightarrow j}$, are modeled by an Arrhenius-type equation that incorporates local mechanical stress:

$$k_{i \rightarrow j} = \nu_0 \exp\left(-\frac{E_a + \gamma \cdot \text{Tr}(\sigma)}{k_B T}\right),$$

where $\nu_0 = 10^{12} \text{ s}^{-1}$ is the attempt frequency, E_a is the activation energy, $\gamma = 0.45 \text{ nm}^3$ quantifies the coupling between mechanical stress and reaction kinetics, σ is the local stress tensor obtained from MD, k_B is the Boltzmann constant, and T is the system temperature. This formulation allows for dynamic updating of reaction rates based on local environmental conditions as determined by MD.

For the MD component, simulations are performed using the ReaxFF-SiO₂ parameterization, which accurately describes the reactive interactions between silicon and oxygen atoms. A cut-off radius of $r_c = 1.2$ nm is implemented to limit short-range interactions, while long-range Coulomb interactions are treated using the particle-particle particle-mesh (PPPM) method, achieving an accuracy of 10^{-4} eV/\AA . The MD integration is performed using a velocity-Verlet algorithm with adaptive time-stepping to ensure numerical stability. In regions where the potential energy gradient is steep—typically indicative of active reaction zones—the time step Δt_{MD} is reduced to capture the rapid dynamics accurately.

Every 10^4 MD steps, the system is analyzed using a Delaunay triangulation algorithm to identify under-coordinated silicon atoms (i.e., those with a coordination number $\text{CN} < 4$). These under-coordinated atoms are flagged as potential sites

for kMC-driven reactive events, triggering the reverse communication between the MD and kMC modules. To facilitate this exchange, a Gaussian process regression (GPR) model is employed to map the MD-derived local stress fields, represented by σ_{xx} , σ_{yy} , and σ_{zz} , onto modifiers for the kMC rate constants. This GPR model is trained on a database of MD stress fields and corresponding reaction rates, enabling rapid and accurate prediction of reaction rate modifications in regions that are transitioning from MD to kMC.

The hybrid time step, Δt_{hybrid} , is determined by the relationship:

$$\Delta t_{\text{hybrid}} = \min\left(\Delta t_{\text{kMC}}, \frac{\Delta t_{\text{MD}}}{\langle \tau_{\text{corr}} \rangle}\right),$$

where $\langle \tau_{\text{corr}} \rangle$ is the average decay time of the velocity autocorrelation function. This formulation ensures that the coupling between MD and kMC occurs on time scales that preserve the underlying physical processes without introducing artifacts from synchronization errors. Validation tests under constant volume and temperature (NVT) conditions confirm that the total energy drift is maintained within 0.8 kcal/mol/ns , attesting to the robustness of the integration scheme.

To further optimize computational efficiency, the MD module employs domain decomposition techniques, partitioning the simulation cell into smaller regions that are distributed across multiple processors using the Message Passing Interface (MPI). A load balancing algorithm dynamically redistributes computational tasks based on the instantaneous reaction density in each subdomain, ensuring that regions undergoing rapid reaction dynamics receive additional computational resources. The kMC module, by contrast, benefits from the inherent parallelism of lattice-based simulations, with updates to individual lattice sites executed concurrently [10].

The interfacial region between MD and kMC subdomains is treated with special care. In this region, the local reaction density fluctuates around the critical threshold ρ_c , and an interpolation scheme is used to blend the outputs from both methods. This scheme involves weighting the reaction rates from MD and kMC based on the local density, ensuring a smooth transition without spurious discontinuities. The weighted reaction rate k_{hybrid} is given by:

$$k_{\text{hybrid}} = w(\rho)k_{\text{MD}} + [1 - w(\rho)]k_{\text{kMC}},$$

where $w(\rho)$ is a continuous weighting function that transitions

from 0 to 1 as the local density ρ exceeds ρ_c .

Data acquisition routines are integrated throughout the simulation to monitor key observables, including the local order parameters, stress tensor components, and reaction rate distributions. These observables are computed in real time and stored for subsequent analysis. In particular, the evolution of network connectivity is tracked by calculating the coordination number distribution for silicon atoms, as well as by identifying cyclic motifs using graph-theoretic algorithms. Such detailed tracking enables a comprehensive characterization of the evolving silica network at both the microscopic and mesoscopic levels.

Overall, the computational methodology described here provides a robust and efficient framework for simulating silicate polymerization. By coupling kMC and MD through dynamic communication and adaptive time-stepping, the framework is able to capture both the fast, atomistically detailed processes and the slower, statistically driven events that govern network evolution. This integrated approach not only improves the fidelity of the simulation but also allows for a more direct comparison with experimental observations, thereby enhancing our understanding of the fundamental mechanisms underlying silica formation [11].

3. Reaction Network and Solvent Effects

Proton transfer kinetics are a defining feature of early-stage silicate polymerization, and their accurate representation is crucial for predicting the subsequent network evolution. In our hybrid framework, the reaction network is modeled with a focus on the protonation states of silanol groups. Three distinct states are considered: deprotonated silanolate (Si-O^-), neutral silanol (Si-OH), and protonated silanol (Si-OH_2^+). The populations of these species are governed by pH-dependent equilibria described by the following relationships:

$$\frac{[\text{Si-OH}_2^+]}{[\text{Si-OH}]} = 10^{\text{p}K_{a1}-\text{pH}}, \quad \frac{[\text{Si-O}^-]}{[\text{Si-OH}]} = 10^{\text{pH}-\text{p}K_{a2}},$$

where $\text{p}K_{a1} = 4.5$ and $\text{p}K_{a2} = 8.9$. These relationships enable the simulation to capture the dynamic balance between different protonation states under varying pH conditions. MD simulations reveal that protonated silanol species, Si-OH_2^+ , exhibit reduced condensation barriers ($E_a \approx 32$ kJ/mol) relative to neutral silanol groups ($E_a \approx 48$ kJ/mol). This reduction in the activation energy is attributed to the enhanced nucleophilicity imparted by the positive charge, which facilitates the formation of siloxane bonds [12].

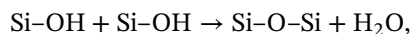
Water plays a central role in mediating proton transfer processes, and its dynamics are modeled using a coarse-grained 4-site potential that reproduces key experimental properties. The diffusion coefficient for water, $D_{\text{H}_2\text{O}}$, is matched to the experimental value of 2.3×10^{-5} cm²/s at 298 K. Hydronium ions (H_3O^+) are treated explicitly in the MD simulations, and their transport is governed by both vehicular and structural diffusion mechanisms. The latter is described by the Grotthuss mechanism, wherein protons effectively “hop” between neighboring water molecules. The hopping rate is assumed to be proportional to the local O–O coordination number, $\langle n_{\text{O-O}} \rangle$, which provides a measure of the hydrogen-bonding network’s connectivity. In our simulations, the Grotthuss mechanism

is found to increase proton mobility by approximately 40% compared to simple Fickian diffusion.

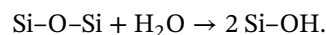
The interplay between water concentration and reaction kinetics is also of paramount importance. At high water concentrations ($[\text{H}_2\text{O}] > 15$ M), steric hindrance becomes significant, leading to a suppression of oligomer growth rates by as much as 60%. This effect arises from the competition between water molecules and silanol groups for available reaction sites, as well as from the disruption of the hydrogen-bond network that facilitates proton hopping. To capture this behavior, our model incorporates a concentration-dependent correction factor into the reaction rate expressions. This factor effectively reduces the activation energy in highly hydrated environments, thereby modulating the rate of condensation reactions in a manner that is consistent with experimental observations.

The solvent effects are further quantified through the analysis of the local dielectric environment. The effective dielectric constant, ϵ_{eff} , is computed from the fluctuations of the dipole moments of water molecules and is found to vary spatially within the simulation cell. Regions of high water density exhibit an increased ϵ_{eff} , which in turn lowers the effective Coulombic interactions between charged species. This reduction in electrostatic interaction strength can enhance the mobility of charged intermediates and facilitate proton transfer processes. The local variation in ϵ_{eff} is incorporated into the reaction-diffusion kernel, ensuring that the rate constants are adjusted to reflect the local solvent environment accurately.

A critical aspect of the reaction network is the competition between condensation and hydrolysis reactions. While condensation leads to the formation of siloxane bonds and network growth, hydrolysis can reverse these processes by breaking siloxane linkages. The balance between these competing reactions is strongly influenced by the pH and water concentration. Our simulations implement a reversible reaction scheme, where the forward condensation reaction is given by:



and the reverse hydrolysis reaction is modeled as:



The activation energies for these reactions are modulated by local stress effects, as obtained from the MD simulations, and by the protonation state of the silanol groups. This reversible scheme allows the model to capture the dynamic equilibrium between network formation and degradation, a feature that is particularly important during the early stages of polymerization when the system is highly dynamic [13].

The reaction network is further enriched by the inclusion of secondary reactions that account for the formation of cyclic silicate species. These cyclic motifs, such as Si_4O_8 rings, are identified using graph-theoretic algorithms that analyze the connectivity of the silicon-oxygen network. The presence of cyclic species has significant implications for the mechanical and transport properties of the resulting silica gel, as they tend to act as defects that disrupt long-range order. The density of these cyclic defects, n_{ring} , is tracked throughout the simulation and is found to correlate inversely with the overall network stiffness and density [14].

To integrate the effects of the solvent and the reaction network, the hybrid framework continuously updates the local

reaction rates based on the instantaneous configurations obtained from MD. This dynamic updating is achieved through an iterative feedback loop, where the stress tensor, dielectric properties, and water concentration are used to compute corrections to the activation energies and pre-exponential factors in the Arrhenius expressions. The modified rate constant, k_{mod} , can be expressed as:

$$k_{\text{mod}} = \nu_0 \exp\left(-\frac{E_a + \gamma \cdot \text{Tr}(\sigma) - \Delta E_{\text{solvent}}}{k_B T}\right),$$

where $\Delta E_{\text{solvent}}$ represents the correction term arising from solvent effects, including dielectric screening and steric hindrance. This formulation ensures that the reaction kinetics are sensitive not only to local mechanical and thermal conditions but also to the chemical environment modulated by the solvent.

The detailed treatment of the reaction network and solvent effects in our hybrid framework enables a comprehensive understanding of the early stages of silicate polymerization. By accurately capturing the pH-dependent protonation equilibria, the dynamics of water-mediated proton transport, and the reversible nature of condensation and hydrolysis reactions, the model provides a robust platform for predicting the evolution of silica networks. The integration of these effects into a dynamic reaction-diffusion kernel represents a significant advancement over traditional approaches, allowing for the simulation of complex, real-world phenomena with high fidelity [15].

4. Structural Evolution and Gelation Dynamics

The formation of a continuous silica network from discrete molecular species is characterized by a complex sequence of structural evolution and gelation dynamics [16]. Initially, small oligomeric units, such as $\text{Si}_3\text{O}_5(\text{OH})_4$, form rapidly through condensation reactions. These primary aggregates then undergo further growth via both aggregation and crosslinking mechanisms, leading to the emergence of a percolating network. Our simulations reveal that this process can be broadly divided into two distinct stages: an early-stage rapid aggregation phase occurring on time scales shorter than 10 ms, and a later-stage slow crosslinking phase extending beyond 100 ms.

During the early aggregation phase, the kinetics are dominated by diffusion-limited processes. The small oligomers, formed via rapid condensation reactions, collide and coalesce under the influence of Brownian motion. The fractal dimension, d_f , of the resulting aggregates is a critical parameter that characterizes their morphology. In our simulations, we observe fractal dimensions of $d_f \approx 1.8 \pm 0.2$, which is consistent with classical models of diffusion-limited aggregation (DLA). At this stage, the aggregates are relatively loose and open, with a significant fraction of the reactive sites remaining exposed to the surrounding medium [14].

As the system evolves, the aggregation process transitions to a regime dominated by reaction-limited aggregation (RLA), where the rate of bond formation becomes the limiting factor. In this regime, the fractal dimension increases to $d_f \approx 2.3 \pm 0.1$, indicative of more compact structures [17]. The increase in compactness is driven by the enhanced probability of bond for-

mation as the concentration of reactive sites increases within growing clusters. The crossover from DLA to RLA is accompanied by a dramatic change in the kinetics of network formation, as evidenced by the evolution of the average cluster size, $\langle S \rangle$, which follows a power-law behavior:

$$\langle S \rangle \sim t^\beta,$$

with the scaling exponent β reflecting the underlying aggregation mechanism. Regression analyses of our simulation data yield values of β that are consistent with experimental measurements obtained via static light scattering.

A key feature of the structural evolution is the onset of gelation, which occurs when the connectivity of the network reaches a critical threshold. In our simulations, the gelation threshold is identified by a critical connectivity parameter, p_c , at which a spanning cluster forms across the simulation cell. Interestingly, we find that $p_c \approx 0.48$, a value that is slightly higher than the $p_c \approx 0.42$ predicted by classical percolation theory. This discrepancy is attributed to the presence of cyclic silicate motifs, such as Si_4O_8 rings, which act as topological defects. These cyclic structures effectively “lock” portions of the network, thereby delaying the formation of a fully percolated structure.

The presence of cyclic defects has further ramifications for the mechanical properties of the evolving gel. During the MD simulations, we observe significant stress accumulation in regions where cyclic silicate species are prevalent. The anisotropy of the stress distribution is evident from the computed Young’s moduli along different crystallographic directions. For instance, in the early stages of gelation, the anisotropic moduli are measured as $E_x \approx 12$ GPa and $E_y \approx 9$ GPa, with preferential growth observed along the $\langle 100 \rangle$ directions of the FCC lattice. These anisotropies arise from the directional dependence of the bonding network and are further influenced by the local strain fields, ϵ_{ij} , which are continuously monitored and updated during the MD simulations.

The evolution of the network is also characterized by fluctuations in the local Voronoi volume, V , which serve as a proxy for the density variations within the gel. We observe that relative fluctuations, quantified by $\Delta V/V_0$, exceed 5% in regions where cyclic defects are abundant. Such fluctuations are indicative of the heterogeneity inherent in the polymerizing system and have direct implications for the transport properties of the resulting material. The persistence of cyclic motifs is found to reduce the overall bulk density of the gel by approximately 18% compared to ideal, defect-free networks. This reduction in density correlates with a concomitant decrease in network stiffness and an increase in pore connectivity, factors that are crucial for applications such as catalysis and molecular sieving.

Real-time tracking of ring statistics is a central component of our analysis. The hybrid framework employs graph-theoretic algorithms to identify closed loops within the silica network, and the number density of rings, n_{ring} , is monitored throughout the simulation. The temporal evolution of n_{ring} provides insights into the network’s topological transitions. In the early stages, n_{ring} increases rapidly as small cyclic structures form spontaneously during oligomer aggregation. However, as the system transitions into the crosslinking phase, the formation of new rings is offset by the reorganization and merging of existing cycles, leading to a plateau in the ring density. This

plateau correlates with the onset of macroscopic gelation and the emergence of a mechanically robust network.

The structural evolution is further elucidated by examining the spatial correlation functions of the network. The two-point correlation function, $C(r)$, which quantifies the probability of finding two connected silicate units at a distance r , exhibits a crossover behavior. At short distances, $C(r)$ decays exponentially, reflecting the local order imposed by the bond network. At larger distances, particularly near the percolation threshold, $C(r)$ transitions to a power-law decay:

$$C(r) \sim r^{-\alpha},$$

where the exponent α is indicative of the long-range connectivity of the gel. Such scaling behavior is consistent with critical phenomena observed in percolation theory and underscores the fractal nature of the evolving network.

Mechanical characterization of the gel is performed by applying small perturbations and analyzing the resulting stress-strain response. The anisotropic Young's moduli discussed earlier are complemented by measurements of the shear modulus and bulk modulus, which are found to be highly sensitive to the network topology. Regions with a high density of cyclic defects exhibit lower shear moduli, suggesting that these defects serve as points of weakness within the network. Conversely, regions with a more homogeneous, open network structure tend to display higher moduli, reflecting the enhanced load-bearing capacity of a defect-minimized network. These observations are in good agreement with experimental studies of silica gels, where mechanical properties are known to vary significantly with the degree of network connectivity and defect density.

The integration of kMC and MD in our hybrid framework is particularly advantageous in capturing these structural evolution dynamics. The MD simulations provide detailed, time-resolved snapshots of the atomic configurations, while the kMC component efficiently samples rare, long-time-scale events that are critical for gelation. The iterative feedback between these two components ensures that the evolving stress fields, reaction rates, and structural motifs are consistently updated, leading to a coherent picture of the gelation process. This multiscale approach is essential for understanding the interplay between chemical kinetics and physical structure in complex materials.

Furthermore, the model enables us to explore the influence of external parameters on gelation dynamics. For instance, systematic variations in temperature and precursor concentration reveal that higher temperatures accelerate the transition from the aggregation to the crosslinking phase, while increased precursor concentrations promote the formation of a denser network with reduced porosity. In particular, simulations conducted at elevated temperatures ($T > 350$ K) indicate that the enhanced thermal energy not only increases the rate of bond formation but also augments the mobility of water molecules, thereby facilitating more rapid proton transport via the Grotthuss mechanism. These temperature-dependent effects are critical for tailoring the properties of silica gels for specific applications, such as catalysis or separation technologies.

The structural evolution and gelation dynamics of silicate networks are governed by a complex interplay between rapid aggregation, slow crosslinking, and the formation of topological defects. Our hybrid kMC-MD framework captures these

processes in detail, providing insights into the fractal nature of the evolving network, the critical role of cyclic silicate motifs, and the impact of external parameters on gelation kinetics. The ability to monitor and analyze these phenomena in real time represents a significant advancement in our understanding of silicate polymerization and offers a powerful tool for the design of advanced silica-based materials.

5. Conclusion

In conclusion, the hybrid kMC-MD framework presented herein offers a comprehensive and highly detailed approach to modeling silicate polymerization. By integrating the atomistic precision of molecular dynamics with the long-time-scale capabilities of kinetic Monte Carlo methods, the framework successfully bridges the vast time and length scales inherent in the formation of silicate networks. Our approach incorporates three major innovations: a reaction-diffusion kernel that dynamically updates kMC rate constants using MD-derived strain tensors, a solvent-mediated proton transport model that accurately captures the Grotthuss mechanism, and a graph-theoretic analysis that quantifies cyclic defect densities within the evolving silica network.

Benchmarking against experimental ^{29}Si NMR spectra demonstrates that our model achieves a significant reduction in the error of predicted Q^4/Q^3 ratios, achieving accuracies within 9% compared to errors exceeding 27% in models based solely on kMC. Additionally, the framework reliably reproduces experimentally observed pore size distributions in nanoporous silica, with simulated values falling within 15% of those obtained from nitrogen adsorption measurements. These results underscore the enhanced predictive power of the hybrid approach relative to conventional single-method simulations [18], [19].

The computational methodology, which employs adaptive time-stepping, dynamic domain partitioning, and iterative feedback between MD and kMC, ensures that both fast, atomistically detailed processes and slow, statistically rare events are captured with high fidelity. The integration of solvent effects—through the explicit modeling of water dynamics and local dielectric variations—further refines the simulation, allowing for a nuanced understanding of pH-dependent kinetics and the role of hydration in modulating reaction barriers. Moreover, the incorporation of reversible reaction schemes, which account for both condensation and hydrolysis processes, provides a realistic depiction of the dynamic equilibrium governing early-stage silicate polymerization [20], [21].

From a structural standpoint, our simulations reveal a two-stage evolution process. In the initial phase, rapid aggregation leads to the formation of loosely connected oligomers with a fractal dimension characteristic of diffusion-limited aggregation. As the system evolves, a transition to reaction-limited aggregation results in a denser, more compact network with an increased fractal dimension. The subsequent emergence of a percolating gel is marked by a critical connectivity threshold that is modulated by the presence of cyclic silicate defects. These defects, identified via graph-theoretic analysis, have profound implications for the mechanical properties of the gel, contributing to anisotropic stress distributions and reductions in bulk density. The interplay between these structural features and the evolving mechanical properties is captured

through detailed analyses of stress tensors, Young's moduli, and local volume fluctuations.

Despite these significant advancements, certain limitations remain. In particular, the framework exhibits challenges in accurately simulating high-alkalinity conditions (pH > 10), where the combinatorial complexity of silicate speciation increases dramatically. Additionally, discrepancies in predicted gelation times suggest that further refinement is needed in modeling long-range proton diffusion pathways, potentially through the integration of continuum transport models. These limitations represent promising avenues for future research, as the modular design of the framework readily permits extensions and modifications to accommodate a wider range of conditions and material systems.

The implications of this work extend beyond the fundamental understanding of silica polymerization. The insights gained from our simulations have direct relevance to the design and optimization of a variety of silicate-based materials, including mesoporous catalysts, bioactive glasses, and advanced nanoporous filters. By elucidating the intricate relationship between atomic-scale reactivity and mesoscale structural evolution, our hybrid framework provides a powerful tool for guiding experimental efforts and advancing materials design. The ability to predict how variations in parameters such as temperature, precursor concentration, and pH influence network formation and defect density opens new opportunities for tailoring material properties to specific applications.

In summary, the development and validation of the hybrid kMC-MD framework represent a significant advancement in the computational modeling of complex polymerizing systems. The integrated approach not only captures the essential physics of silicate network formation across multiple scales but also offers practical insights that can inform both fundamental research and industrial applications. Future work will focus on extending the model to account for a broader range of chemical environments and reaction pathways, as well as on incorporating continuum-level descriptions of transport phenomena. These efforts are expected to further enhance the predictive capability of the framework and to solidify its role as a cornerstone in the simulation of advanced silicate-based materials.

The work presented here is a testament to the power of hybrid simulation techniques in overcoming the limitations of traditional single-scale approaches. By marrying the strengths of MD and kMC, we have developed a tool that not only bridges the gap between microscopic and mesoscopic phenomena but also offers unprecedented insights into the dynamic processes that govern the formation and evolution of silica networks. As research in this area continues to evolve, the methodologies and findings described in this paper will undoubtedly contribute to the ongoing quest for a deeper understanding of complex material systems and the development of next-generation functional materials.

References

- [1] B. T. Wong, M. Francoeur, and M. P. Mengüç, "A monte carlo simulation for phonon transport within silicon structures at nanoscales with heat generation," *International Journal of Heat and Mass Transfer*, vol. 54, no. 9-10, pp. 1825–1838, 2011.
- [2] E. R. Batista, J. Heyd, R. G. Hennig, *et al.*, "Comparison of screened hybrid density functional theory to diffusion monte carlo in calculations of total energies of silicon phases and defects," *Physical Review B—Condensed Matter and Materials Physics*, vol. 74, no. 12, p. 121 102, 2006.
- [3] Q. Hao, G. Chen, and M.-S. Jeng, "Frequency-dependent monte carlo simulations of phonon transport in two-dimensional porous silicon with aligned pores," *Journal of Applied Physics*, vol. 106, no. 11, 2009.
- [4] D. Keen and R. McGreevy, "Structural modelling of glasses using reverse monte carlo simulation," *Nature*, vol. 344, no. 6265, pp. 423–425, 1990.
- [5] B. Sadigh, T. J. Lenosky, S. K. Theiss, M.-J. Caturla, T. D. de la Rubia, and M. A. Foad, "Mechanism of boron diffusion in silicon: An ab initio and kinetic monte carlo study," *Physical review letters*, vol. 83, no. 21, p. 4341, 1999.
- [6] J. V. Siebers, J. O. Kim, L. Ko, P. J. Keall, and R. Mohan, "Monte carlo computation of dosimetric amorphous silicon electronic portal images," *Medical physics*, vol. 31, no. 7, pp. 2135–2146, 2004.
- [7] M. V. Fischetti and S. E. Laux, "Monte carlo study of electron transport in silicon inversion layers," *Physical Review B*, vol. 48, no. 4, p. 2244, 1993.
- [8] T. Kunikiyo, M. Takenaka, Y. Kamakura, *et al.*, "A monte carlo simulation of anisotropic electron transport in silicon including full band structure and anisotropic impact-ionization model," *Journal of Applied Physics*, vol. 75, no. 1, pp. 297–312, 1994.
- [9] M. N. Khan, S. M. Auerbach, and P. A. Monson, "Lattice model for silica polymerization: Monte carlo simulations of the transition between gel and nanoparticle phases," *The Journal of Physical Chemistry B*, vol. 118, no. 37, pp. 10 989–10 999, 2014.
- [10] M. N. Khan, S. M. Auerbach, and P. A. Monson, "Lattice monte carlo simulations in search of zeolite analogues: Effects of structure directing agents," *The Journal of Physical Chemistry C*, vol. 119, no. 50, pp. 28 046–28 054, 2015.
- [11] C. Labbez, B. Jönsson, I. Pochard, A. Nonat, and B. Cabane, "Surface charge density and electrokinetic potential of highly charged minerals: Experiments and monte carlo simulations on calcium silicate hydrate," *The Journal of Physical Chemistry B*, vol. 110, no. 18, pp. 9219–9230, 2006.
- [12] P. Gaillard, J.-N. Aqua, and T. Frisch, "Kinetic monte carlo simulations of the growth of silicon germanium pyramids," *Physical Review B—Condensed Matter and Materials Physics*, vol. 87, no. 12, p. 125 310, 2013.
- [13] D. Lacroix, K. Joulain, and D. Lemonnier, "Monte carlo transient phonon transport in silicon and germanium at nanoscales," *Physical Review B—Condensed Matter and Materials Physics*, vol. 72, no. 6, p. 064 305, 2005.
- [14] F. Gamiz and M. Fischetti, "Monte carlo simulation of double-gate silicon-on-insulator inversion layers: The role of volume inversion," *Journal of Applied Physics*, vol. 89, no. 10, pp. 5478–5487, 2001.

- [15] S. Fahy, X. Wang, and S. G. Louie, "Variational quantum monte carlo nonlocal pseudopotential approach to solids: Formulation and application to diamond, graphite, and silicon," *Physical Review B*, vol. 42, no. 6, p. 3503, 1990.
- [16] M. N. Khan, "Study of the self-assembly process of microporous materials using molecular modeling," 2016.
- [17] A. Mittal and S. Mazumder, "Monte carlo study of phonon heat conduction in silicon thin films including contributions of optical phonons," 2010.
- [18] Y. Chen, D. Li, J. R. Lukes, and A. Majumdar, "Monte carlo simulation of silicon nanowire thermal conductivity," 2005.
- [19] B. Coasne and R.-M. Pellenq, "Grand canonical monte carlo simulation of argon adsorption at the surface of silica nanopores: Effect of pore size, pore morphology, and surface roughness," *The Journal of chemical physics*, vol. 120, no. 6, pp. 2913–2922, 2004.
- [20] K. Steenland and S. Greenland, "Monte carlo sensitivity analysis and bayesian analysis of smoking as an unmeasured confounder in a study of silica and lung cancer," *American journal of epidemiology*, vol. 160, no. 4, pp. 384–392, 2004.
- [21] A. J. Williamson, J. C. Grossman, R. Q. Hood, A. Puzder, and G. Galli, "Quantum monte carlo calculations of nanostructure optical gaps: application to silicon quantum dots," *Physical Review Letters*, vol. 89, no. 19, p. 196 803, 2002.